Magnesium Technology 2012
Edited by: Suveen N. Mathaudhu, Wim H. Sillekens, Neale R. Neelameggham, and Norbert Hort
TMS (The Minerals, Metals & Materials Society), 2012

EFFECT OF CORROSION ON THE TENSILE PROPERTIES OF FRICTION-STIR WELDED AZ31B SHEET

Jennifer M. Thuss, Joseph R. Kish, Joseph R. McDermid
Centre for Automotive Materials and Corrosion, McMaster University, Hamilton, ON L8S 4L7

Keywords: Friction stir welding; Magnesium alloys; Residual stress; Scanning electrochemical measurements

Abstract

To facilitate the use of magnesium and its alloys within automotive structures, it is necessary to characterize their possible mechanical property degradation in typical application environments. This work examines the effect of exposure to NaCl-based corrosive environments on the mechanical properties of friction stir welded (FSW) AZ31B magnesium alloy sheet. A complete microstructural, electrochemical, residual stress and mechanical property characterization of the as-received FSW panels was performed. Samples were subsequently exposed to 0.01 M and 0.1 M NaCl solutions at the corrosion potential for 24 h and any changes in mechanical properties, as a function of exposure, to the corrosive environment monitored. Friction stir welded panels exhibited large decreases in ductility compared to the base AZ31B material. Exposure to 0.1 M NaCl for 24 hours resulted in a degradation in mechanical properties for the base material, as well as the friction stir welded panel, whereas no significant changes were found for samples exposed to 0.01 M NaCl for 24 hours.

Introduction

Magnesium alloys are promising candidates for use as structural components in the automotive and aerospace industries due to their relatively high specific strength. To facilitate the use of magnesium alloys within automotive structures, it is necessary to characterize the possible mechanical property degradation in typical application environments [1]. These components can be joined using welding techniques such as metal inert gas welding (MIG), tungsten inert gas welding (TIG) and friction stir welding (FSW), and so it is also critical to assess the combined effects of welding and exposure to corrosive environments on possible mechanical property degradation.

Friction stir welding is a relatively new solid state joining technique that creates a weld bead with limited to no porosity within the weld or heat affected zone (HAZ) [3]. This technique was originally designed for use with aluminum alloys, however magnesium alloys have been successfully welded using this technique [4]. One of the many advantages to using FSW is that the weld zone, created below the melting point of the material, contains fine equiaxed grains [3]. This is due to the rapid dynamic recrystallization that occurs during the welding process. FSW process parameters such as tool rotation speed, tool geometry and tool transverse speed are critical to the evolution of weld microstructures and properties [3].

The objective of the present study is to examine the effect of FSW on the mechanical properties of AZ31B sheet, both in the unexposed condition and after exposure to 0.01 M and 0.1 M NaCl solutions at room temperature.

Experimental Procedures

Material

The experimental materials comprised 2 mm thick wrought AZ31B magnesium alloy sheet. The sheets were hot rolled and partially annealed to the H24 condition. The composition of the AZ13B sheet was analyzed using standard wet chemistry techniques and Inductively Coupled Plasma Optical Emission Spectroscopy (ICP-OES), the results of which are shown in Table I.

Table I: ICP-OES Analysis of Material Composition

Element (in wt%)						
Al	Zn	Mn	Fe	Si	Ni	Ca
2.938	1.103	0.448	0.005	0.005	0.001	0.001

Prior to fabricating the FSW joints, a steel brush was used to remove any surface oxide present on the AZ31B sheet. A final cleaning step using ethanol wiping was conducted prior to welding. A H13 steel tool with a 9.5 mm shoulder and 3.175 mm left-handed pin was used to weld all sample panels. Welding was completed under position control with a tilt angle of 0.5°. All friction stir welds were fabricated using a rotation speed of 1000 rpm and a transverse speed of 5 mm/s.

Microstructure Characterization

Weld sections were cross-sectioned and cold mounted in epoxy resin. Samples were then polished to 4000 grit SiC paper. The samples were then electrolytically polished using a solution of 3 parts phosphoric acid (85%) and 5 parts ethanol (100%) maintained at 2°C and stirred vigorously. The sample was subjected to a 2 V potential for 120 s, followed by 1.5 V for 120 s. The sample was then chemically etched for 3 s in an acetic picral solution containing 2.1 g picric acid, 5 mL acetic acid and 80 mL ethanol (95%). Optical microscopy of the weld microstructure was conducted using a Nikon Eclipse LV100 microscope.

Tensile Tests

Sub-size tensile specimens conforming to ASTM B557 [5] were machined perpendicular to the weld direction for each panel. Specimens were tested in a variety of environmental exposure conditions in order to characterize possible mechanical property degradation. The environmental conditions used were; unexposed and 24 h pre-exposure to room temperature 0.1 M NaCl and 0.01 M NaCl solutions at the corrosion potential. All tensile specimens were tested to fracture at a strain rate of 5.5×10^{-5} s^{-1} using a standard tensile frame equipped with a 10 kN load cell. Digital image correlation techniques were utilized to calculate strain as a function of time. Tensile sample fracture surfaces were examined using a Philips 515 scanning electron microscope at an acceleration voltage of 15 keV.

Scanning Electrochemical Measurements

The electrochemical behavior of the weld cross-section was analyzed using a M370 scanning electrochemical workstation and PG580R Potentiostat. Potentiodynamic polarization experiments were completed on a number of micro-sections of the weld region, HAZ and base material at a scan rate of 5 mV/s in a 0.1 M NaCl solution at room temperature. These experiments were conducted using a stationary PTFE droplet cell with a 1 mm diameter probe tip. This M370 scanning droplet system (SDS) module is fit with a platinum counter electrode and an Ag/AgCl reference electrode.

Residual Stress Analysis

A 2D X-ray diffractometer, using Cu $K_{\alpha 1}$ radiation, was used to collect residual stress information from six points within the weld cross section. To conduct this analysis a 20 mm section was cut from the welded panel. The data was then analyzed using GADDS software. It is important to note that cutting the specimen might have allowed for relaxation of the residual stresses present. The trends in tensile versus compressive residual stress were the focus of this experiment, however.

Results and Discussion

Microstructure

Optical images of the microstructure of the stir zone, apparent HAZ and base material are shown in Figure 1 a) – c), respectively.

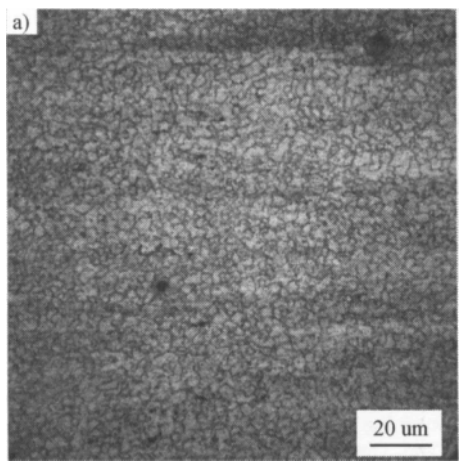

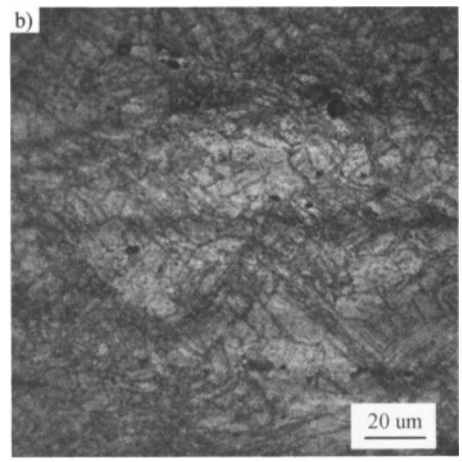

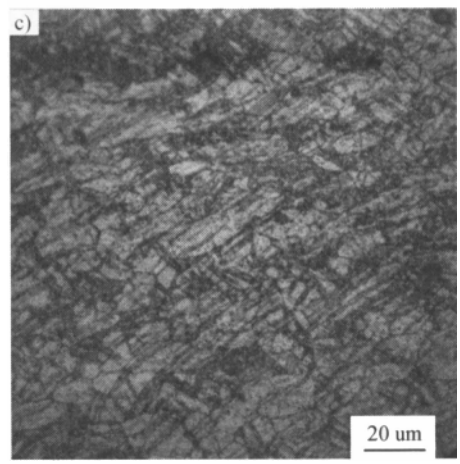

Figure 1: Microstructure of a) stir zone (x = 0 μm) b) apparent HAZ (x = 6500 μm) and c) base material (x = 20,000 μm)

It is clear that the microstructure within the stir zone consisted of fine recrystallized grains due to the friction stir welding process. Both the HAZ and base material exhibited a larger grain size, which contained twins [6]. The presence of twins within the HAZ is believed to be caused by the alloy manufacture as there was no significant difference between HAZ and base material microstructures. This lack of significant HAZ microstructure difference may have arisen from the relatively low heat input for these welding parameters.

Mechanical Properties

Results of the tensile tests for both the base and FSW AZ31B are shown in the form of true stress-strain curves in Figure 2. A summary of the mechanical properties for the base and FSW AZ31B as a function of exposure condition is shown in Table II.

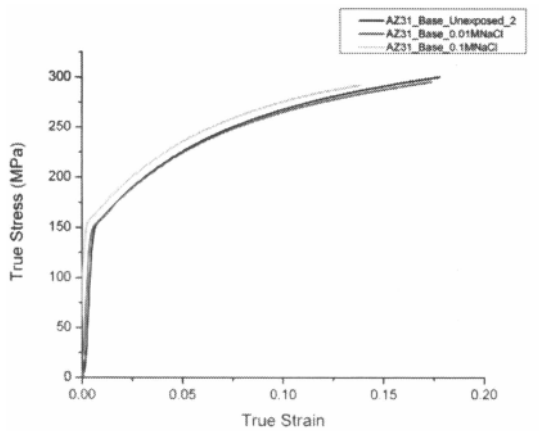

a) Base AZ31B

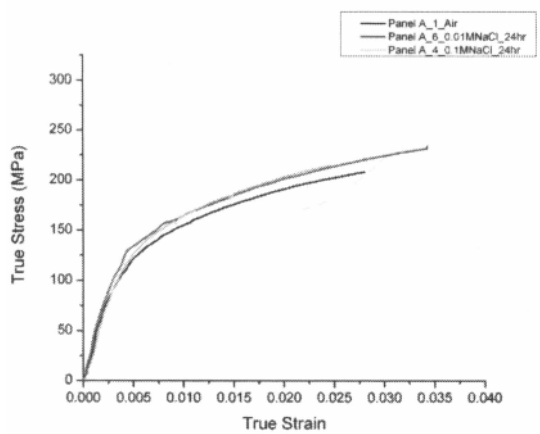

b) Friction stir welded AZ31B

Figure 2: True stress-true strain curves of base and FSW AZ31B in various environments. Note the change in scale for the strain axis between a) and b)

The exposure of base AZ31B to 0.01 M NaCl solution for 24 h at the corrosion potential had no significant effect on the ultimate tensile strength (UTS) or uniform elongation of the material versus the unexposed condition (Figure 2a, Table II). However, exposure to 0.1 M NaCl had a negative impact on the uniform elongation where a decrease in uniform elongation to 14% versus 18% for the base material was observed (Figure 2a, Table II). No significant change in UTS versus the base material was observed for the 0.1 M NaCl exposure. Song et al. found a decrease in ductility and UTS for AZ31 tested in both 0.1 M NaCl and 0.01 M NaCl at a strain rate of 1 x 10^{-6} s^{-1}. Larger decreases in ductility, up to 34%, are thought to be an effect of the in-situ corrosion occurring and slower strain rate [2].

All FSW tensile specimens failed at the interface between the stir zone and HAZ on the retreating side of the weld. A large decrease in uniform elongation was observed for the FSW specimens as compared to the base material (Figure 2a, b, Table II). The friction stir welding process did not have as large of an effect on the UTS; a decrease of approximately 20 MPa was observed (Table II).

Similar to the findings for the base material, exposure to 0.01 M NaCl did not have a significant effect on the tensile properties of the FSW material (Table II).

Table II: Summary of mechanical properties for as-received and welded AZ31B, as a function of exposure condition

Specimen	Uniform Elongation (%)	UTS (MPa)
Base – Unexposed (Average)	17.8	242
Base – 0.01 M NaCl for 24 h	17.4	248
Base – 0.1 M NaCl for 24 h	13.8	254
FSW – Unexposed (Average)	3.0	230
FSW – 0.01 M NaCl for 24 h	3.0	226
FSW – 0.1 M NaCl for 24 h	2.5	217

SEM Fractography

Tensile specimen fracture surfaces were analyzed using a scanning electron microscope. The base material was found to exhibit ductile fracture in the unexposed state (Figure 3a) and exhibited some brittle fracture features in the 0.1 M NaCl exposure condition (Figure 3b). This behavior was expected since a decrease in uniform elongation was observed (Figure 2a, Table II). The FSW specimens displayed brittle and cleavage facets in all exposure conditions (Figure 3c, d), as would be expected from the significant decrease in uniform elongation observed versus the base material (Figure 2b, Table II).

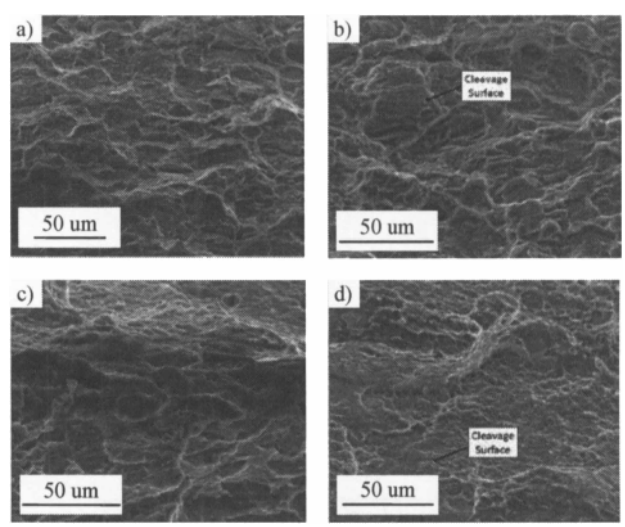

Figure 3: SEM Imaging of a) unexposed base material fracture surface b) base material fracture surface tested after exposure to 0.01 M NaCl solution at the corrosion potential for 24 h c) unexposed FSW material fracture surface and d) FSW material fracture surface tested after exposure to 0.1 M NaCl solution at the corrosion potential for 24 h.

Scanning Electrochemical Measurements

Potentiodynamic polarization scans were completed for 5 micro-sections on a cross-sectioned sample of welded AZ31B. Electrochemical behavior as a function of distance from the weld centerline (x = 0 μm) were recorded and are shown in Figure 4.

Fluctuations within the potentiodynamic polarization scans during the scanning droplet experiment were observed, due to the existence of a short circuit within the electrochemical cell. The cause of this short circuit and effective fluctuation is not confirmed but could be due to air entering the system or by the generation of gas bubbles during corrosion processes [7]. These short instabilities, however, still allow corrosion analyses to be completed. For clarity, the data affected by these fluctuations within the system was not presented.

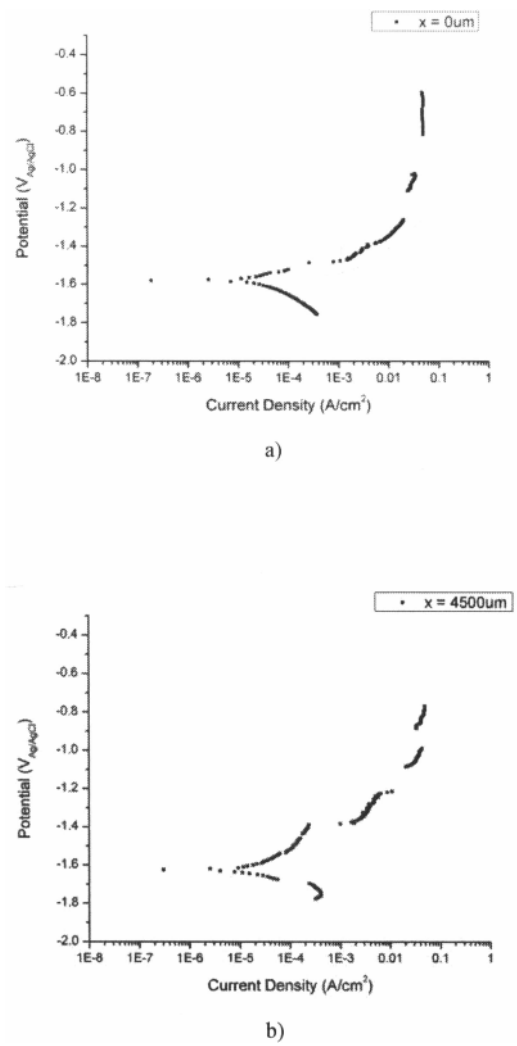

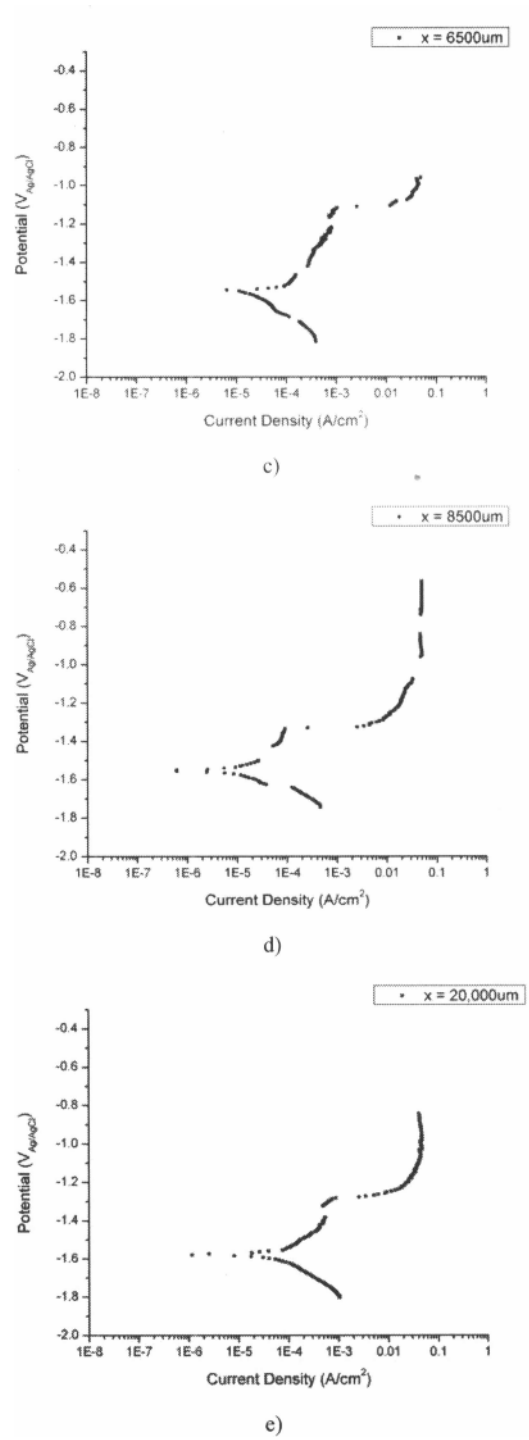

Figure 4: Potentiodynamic behavior of a) stir zone (x = 0μm) b) stir zone edge (x = 4500μm) c) outside edge of stir zone (x = 6500μm) d) HAZ (x = 8500μm) and e) base material (x = 20,000μm).

The data collected from the potentiodynamic scans is summarized in Table III. From this data, it can be seen that there were small variances in corrosion potential and corrosion current density as a function of distance from the weld centerline. All breakdown potentials are more noble than their respective corrosion potentials and all mechanical tests were completed at the corrosion potential. The cathodic exchange current density calculations show that there were no significant differences in the cathodic reaction kinetics across the weld section.

Hydrogen induced cracking and pitting corrosion are two types of corrosion mechanisms that effect mechanical properties. The cathodic hydrogen evolution reaction can cause hydrogen embrittlement which is proposed to aid in the cracking mechanism [8]. Mechanical properties can also be affected by the presence of localized pits which act as stress concentrators [8]. The understanding that there were no significant differences in cathodic kinetics as a function of distance correlates well to the observed mechanical properties. If there was an observed localized cathodic site it would be expected to coincide with the location of fracture due to the effect of hydrogen embrittlement. This is not the case since all tensile specimens failed in the same region on the retreating side of the weld zone. The location of fracture also would (be expected to) have changed if there was an effect of pitting corrosion. Again this is not the case since all tensile specimens were exposed at the corrosion potential, which was less noble than all observed breakdown potentials.

Table III: Electrochemical behavior summary of FSW welded AZ31B.

Position (μm)	E_{CORR} (V)	E_{BK}(V)	i_{CORR} (A/cm^2)	$i_{o,c}$ (A/cm^2)
0	-1.58	-1.49	5.0×10^{-5}	3.6×10^{-10}
4500	-1.63	-1.39	2.0×10^{-5}	4.2×10^{-10}
6500	-1.55	-1.11	1.9×10^{-5}	1.2×10^{-11}
8500	-1.55	-1.33	2.6×10^{-5}	1.7×10^{-10}
20,000	-1.58	-1.28	6.5×10^{-5}	3.0×10^{-10}

Residual Stress Analysis

X-ray analysis was completed on a plane view section of FSW material; a macrograph of this sample is shown in Figure 5.

Figure 5: XRD sample setup and designation

The maximum principle stresses calculated from this experiment are shown in Figure 6. From this analysis it was found that the stir zone contained large tensile residual stresses, ranging from 200 to 150 MPa, moving towards small compressive residual stresses within the HAZ and base material. These residual stresses are present due to the FSW process [9]. Again it is important to take note of the trend that exists for the residual stresses found within the weld versus the magnitude of the stresses calculated.

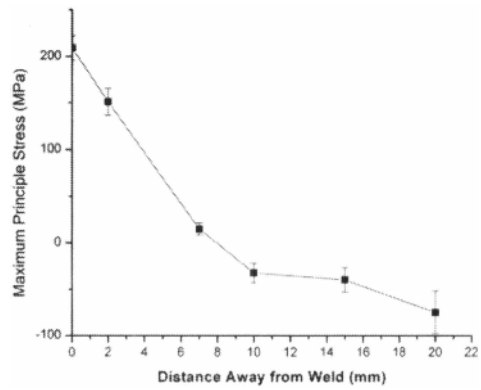

Figure 6: Residual Stress Analysis using 2D X-Ray Diffraction

The large gradient in residual stresses at the interface between the stir zone and HAZ correlates to the tensile specimen fracture that occurs on the edge of the stir zone. This trend is comparable to that found in an aluminum alloy friction stir weld, researched by Prime et al. The 7050-2024 FSW system contained tensile residual stresses within the stir zone, ranging from 30 to 40 MPa, and compressive residual stresses within the base material [9]. The difference in magnitude is assumed to be due to the material system as well as the welding parameters.

Summary

1) The microstructure within the stir zone consisted of fine, re-crystallized grains. Larger grains containing twins were found within the HAZ as well as the base material.
2) A slight decrease in tensile strength and large decrease in ductility were observed for FSW panels, as compared to the base AZ31B material, for all environmental exposure conditions tested.
3) Exposure to 0.01 M NaCl solution for 24 h at room temperature did not have a significant effect on the mechanical properties (UTS, elongation at fracture, etc) for both the base material and the welded panels, whereas degradation in mechanical properties was observed in both materials exposed to 0.1 M NaCl for 24 h at the corrosion potential.
4) No significant relative differences in cathodic and anodic corrosion behaviour were found across the weld section.
5) A transition between tensile residual stress and compressive residual stress exists from the stir zone out to the base material. The location of this transition zone coincides with the fracture location in the FSW joints.

Acknowledgements

The authors would like to thank General Motors for the donation of experimental materials and the National Research Council of Canada for fabrication of the friction stir welded panels. The financial support of the Natural Sciences and Engineering Research Council of Canada (NSERC) is also acknowledged.

References

1. G. Song, and A. Atrens, "Understanding Magnesium Corrosion, A Framework for Improved Alloy Performance," *Advanced Engineering Materials*, 5 (2003), 837-858.

2. R.G. Song, C. Blawert, W. Dietzel, and A. Atrens, "A study on stress corrosion cracking and hydrogen embrittlement of AZ31 magnesium alloy," *Materials Science and Engineering A*, 399 (2005), 308-317.

3. R.S. Mishra and Z.Y. Ma, "Friction stir welding and processing," *Materials Science and Engineering R: Reports*, 50 (2005)

4. R. Johnson. "Friction stir welding of magnesium alloys," *Magnesium Alloys 2003, Pts 1 and 2*, 419-4 (2003), 365-370

5. ASTM Standard B557, 2010. "Standard Test Methods for Tension Testing Wrought and Cast Aluminum- and Magnesium-Alloy Products," ASTM International, West Conshohocken, PA, 2010, DOI: 10.1520/B0557-10, www.astm.org.

6. M.B. Kannan, W. Dietzel, R. Zeng, R. Zettler, and J.F. dos Santos, "A study of the SCC susceptibility of friction stir welded AZ31 Mg sheet," *Materials Science and Engineering A-Structural Materials Properties Microstructure and Processing*, 460 (2007), 243-250.

7. K. Fushimi, S. Yamamoto, R. Ozaki, and H Habazaki, "Cross-section corrosion-potential profiles of aluminum-alloy brazing sheets observed by the flowing electrolyte scanning-droplet-cell technique," *Electrochimica Acta*, 53 (2008), 2529-2537.

8. N. Winzer, A. Atrens, G. Song, E. Ghali, W. Dietzel, K.U. Kainer, "A critical review of the Stress Corrosion Cracking (SCC) of magnesium alloys," *Advanced Engineering Materials*, 7 (2005), 659-693.

9. M.B. Prime, T. Gnaupel-Herold, J.A. Baumann, R.J. Lederich, D.M. Bowden, and R.J. Sebring, "Residual stress measurements in a thick, dissimilar aluminum alloy friction stir weld," *Acta Materialia*, 54 (2006), 4013-4021.